Energy and Exergy Analysis and Selection of the Appropriate Operating Fluid for a Combined Power and Hydrogen Production System Using a Geothermal Fueled ORC and a PEM Electrolyzer

Norouzi, Nima; Fani, Maryam*+

*Department of Energy Engineering and Physics, Amirkabir University of Technology (Tehran Polytechnic),
Tehran, I.R. IRAN*

ABSTRACT: *This research aims to introduce an efficient power cycle that simultaneously produces power and hydrogen in PEM electrolyzer. This cycle is driven by geothermal energy. Comprehensive thermodynamic modeling (energy and exergy) has been performed to compare four different operating fluids' performance in the proposed system. EES software was used for modeling. A parametric study has also been applied to investigate the effect of important parameters on the system's energy and exergy performance. As a brief novelty statement, the unique model can be mentioned in which both power and chemicals can be produced, and hydrogen output can be used as a storage system that transforms energy into an energy carrier. The results showed that R245fa operating fluid with 3.5% and %67.6 of energy and exergy efficiency had the highest performance. The operating fluids R114, R600, and R236fa are also in the next ranks of performance characteristics. As the geothermal fluid temperature increases, the production of power and hydrogen increases, but the energy and exergy efficiency decrease. Also, it can be noted that the hydrogen unit significantly increases the exergy efficiency of the plant. As an example, in the R245fa case, it increases from 36% to 67.6%.*

INTRODUCTION

Today, the energy supply issue from renewable methods has become a basic need, and many countries are looking for renewable methods to produce energy due to the depletion of fossil fuel resources. Geothermal energy is a renewable method with an economically high capacity to generate electricity [1, 2]. Although high-temperature geothermal sources are more economical because most geothermal sources are in the low-temperature range, it is predicted that the next generation of geothermal power plants will use more low-temperature sources [3]. The Organic Rankine Cycle (ORC) is a power generation cycle that can be started using low-temperature energy sources due to low boiling point organic fluids [4].

Hydrogen is considered a clean energy carrier for

environmentally friendly energy production, mainly used in the power plant and chemical industries [5, 6]. Besides, it can be effectively converted to electricity in fuel cell systems with negligible greenhouse effects [7, 8]. Today, hydrogen can be produced through fossil fuel sources, hydrocarbon reforming processes, and water electrolysis. But due to limited fossil fuels and changing climatic conditions due to the release of carbon dioxide and other pollutants, attention has been placed on renewable hydrogen production methods[9]. Meanwhile, water electrolysis is an accepted technology for large-scale hydrogen production. Hydrogen production by electrolysis through proton membrane exchange (PEM) has many advantages, including very low environmental effects and easy maintenance [10]. Cogeneration is one of the best ways to conserve and store energy, allowing efficient energy resources and preserving the environment.

Among different energy sources, geothermal energy has significant potential for hydrogen production. All or part of a geothermal power plant's output power can produce hydrogen through the water electrolysis process. It seems that hydrogen production based on geothermal energy and water electrolysis operation will undeniably affect the economy of hydrogen production [1].

In a combined geothermal cycle using carbon dioxide gas as a heat transfer fluid, *Ahmadi et al.* used electrically decomposing water to produce hydrogen. They performed technical, economic, and environmental analyses on the system and concluded that the electrical system has the highest cost share with more than 90% of the total cost. The cost of hydrogen production is also $ 8.24/kg [5].

Rahmouni et al. worked on a system based on geothermal and solar energy to produce hydrogen. They used solar energy to produce hydrogen and heat and geothermal energy to produce power and cooling. By performing energy, exergy, and parametric analyses on their system, they concluded that at 210 °C, geothermal water, energy, and exergy efficiencies could reach 10.8 and 46.3%, respectively [7]. *Balta et al.* Performed exergy, energy, economic, and mass analyses on a copper-chlorine thermochemical water decomposition system combined with geothermal energy to produce hydrogen. The results showed that the cost of hydrogen production is directly and very closely related to the power plant's capacity and exergy efficiency [9]. In a study, *Qiong et al.* examined the optimal methods for controlling hydrogen production

when an electrolyzer is connected to an alternating renewable energy source and compared the methods' efficiency [10]. In a hydrogen production system with a geothermal source, *Alhamid et al.* Used four different models and two reversible and irreversible modes and performed exergy analysis for all four systems. They concluded that the exergy efficiencies of models 1, 2, 3 and 4 are 28.5%, 29.9%, 37.2% and 16.1%, respectively [1]. In a study by *Mahmoudan et al.* [11], a novel integrated energy system based on a geothermal heat source, and a liquefied natural gas heat sink is proposed for providing heating, cooling, electricity power, and drinking water simultaneously. The arrangement is a cascade incorporating a flash-binary geothermal system, a regenerative organic Rankine cycle, a simple organic Rankine cycle, a vapor-compression refrigeration cycle, a regasification unit, and a reverse osmosis desalination system. Energy, exergy, and exergoeconomic methods are employed to analyze the suggested system. In research by *Hoseinzadeh et al.* [12], the integrated carbon dioxide power cycle with the geothermal energy source to supply the necessary reverse osmosis desalination power for freshwater production is defined. The cycling power is consumed by the desalination system and sodium hypochlorite generator. Exergoeconomic analysis and optimization are studied. Exergoeconomic analysis shows that the desalination system, sodium hypochlorite generator, carbon dioxide turbine, and natural gas turbine have the highest rate of capital gain and exergy destruction cost.

Research done by *Sohani et al.* [13] studied solar irradiation in hot-arid climatic countries results in increased temperatures, one of the major factors affecting the power generation efficiency of monocrystalline photovoltaic (PV) systems, posing performance and degradation challenges. In this paper, the efficiency of a water-flow cooling system to increase the output of a monocrystalline PV module with a rated capacity of 80 W is studied from both energy and exergy perspectives. The energy and exergy tests are performed for each season of the year, with and without cooling. The energy and exergy efficiencies and the commodity exergy values are used to compare the photovoltaic device with and without cooling.

In another study by *Hoseinzadeh* and *Heyns* [14], Energy, Exergy, and Environmental (3E) analysis of a 400 MW thermal power plant is investigated. First, the power plant components are examined in terms of energy

consumption, and subsequently, energy losses, exergy destruction, and energy efficiency are obtained.

In a study by *Kariman et al.* [15], desalination systems are considered promising solutions to deal with the water scarcity problem. Among different kinds of desalination systems, having the advantages like using low-grade thermal resources, the multi-effect type is getting more popular. Considering the mentioned issues, in this study, a high-performance Multi-Effect Desalination (MED) system is introduced and the enhancement potential is evaluated in detail. The introduced and reference designs are compared together from different points of view.

In a study by *Ghazvini et al.* [16], a concise summary of present and advancing hydrogen production technologies are presented, and secondarily a comprehensive review of research associated with hydrogen production based on geothermal energy is provided. Thirdly, the process descriptions of geothermal-assisted hydrogen production and its technical, economic, and environmental aspects are addressed. Finally, comparative assessments of costs and environmental aspects of hydrogen production based on different energy sources have been performed.

In a paper, *Ahmadi et al.* [17], an analysis of energy and exergy thermodynamics and the exergy-economic analysis of the proton exchange membrane (PEM-type) electrolysis process for hydrogen production, which derives its driving power from ground-based power, has been carried out.

In a study by *Ahmadi et al.* [18], a transcritical Carbon dioxide power cycle has been coupled to a liquefied natural gas to work either as the cold source or enhance further to generate electricity. A detailed thermodynamic analysis is performed to investigate the effect of key parameters on the cycle performance. Also, heat exchangers are measured to find the heat transfer surface area for economic evaluation.

A study by *Sadaghiani et al.* [19] proposes a new power generation plant to convert the trapped energies of geothermal hot water and Liquid Natural Gas streams to usable power. The combined power plant consists of 7 units, each unit includes three discrete cycles of Kalina and two Organic Rankine power generation cycles to produce power from its heat sources.

This research investigates power production by an efficient organic Rankin cycle equipped with a heat recovery exchanger (regenerator) and a heating fluid heater. This cycle is driven by geothermal energy. Also

used to produce hydrogen is a proton exchange membrane whose power is supplied through the organic Rankine cycle. The main objectives of this research are: Using geothermal energy as a source of low-temperature energy for the cogeneration of power and hydrogen; Using a modified organic Rankine cycle with four different operating fluids and comparing the introduced system's energy and exergy performance for all operating fluids; Parametric study to investigate the effect of an important parameter on the performance of the hybrid system.

This paper's main novelty is the cycle's unique arrangement and hydrogen production in low-temperature energy systems. And using exergy analysis to investigate this system's performance helps technical experts and policymakers make optimal technology selection decisions [20-24].

THEORETICAL SECTION

In the present work, a modified organic Rankine cycle (equipped with a regenerator and feed fluid heater) is combined with a PEM electrolysis to produce power and hydrogen simultaneously. Fig. 1 shows the schematic of the system under consideration. To model, the system's energy, mass, and energy conservation rules must be applied to each component of the system. For this purpose, each element is considered a control volume [25-30].

$$\sum_i m_i = \sum_e m_e \tag{1}$$

$$Q^. - W^. = \sum_e m_e h_e - \sum_i m_i h_i \tag{2}$$

Exergy [24] is divided into physical exergy, chemical exergy, kinetic exergy, and potential exergy. Due to small changes in speed and altitude, and changes in the chemical composition of flows, the terms kinetics, potential, and chemical exergy have been omitted in this study (chemical exergy is only considered during the fuel cell process). Physical exergy is considered the maximum useful work of the theory obtained by the system in interaction with the environment in equilibrium conditions [25]. Considering the first and second laws of thermodynamics, the exergy balance can be considered as follows.

$$Ex_Q^. + \sum_i m_i ex_i = \sum_e m_e ex_e + Ex_W^. + Ex_D \tag{3}$$

Indices i and e specify the input and output exergy to the control volume. Ex_D represents exergy destruction, and the other terms are determined by Eqs. (4-6).
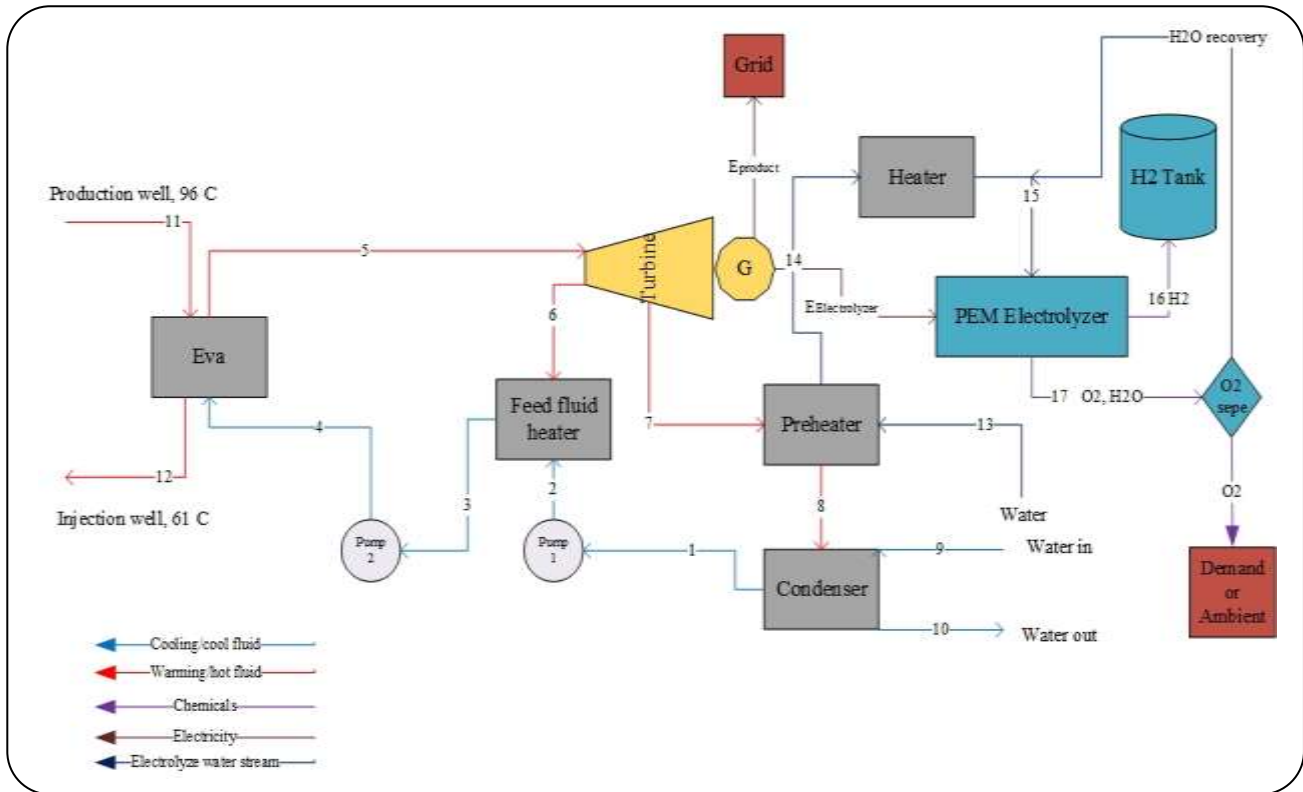
Fig. 1: Rankine organic cycle diagram equipped with heat recovery exchanger (regenerator) and feed fluid heater combined with geothermal energy of proton membrane exchange electrolyzer.

$$Ex_Q = \left(1 - \frac{T_0}{T_i}\right) Q_i \tag{4}$$

$$Ex_W = W^{\cdot} \tag{5}$$

$$ex = ex_{ph} = (h - h_0) - T_0(s - s_0) \tag{6}$$

The energy efficiency of the cogeneration system under consideration is calculated based on Eq. (7) [25-29].

$$\eta_{th} = \frac{W_{net} + Q_{heating}}{Q_{Recovery} + Q_{Geothermal}} \tag{7}$$

$$Q_{brine} = m_9(h_{10} - h_9) + m_{11}(h_{12} - h_{11}) \tag{8}$$

$$W_{net} = W_{turbine} - W_{pumps} \tag{9}$$

The exergy efficiency of the cogeneration system is obtained based on Eq. (10) [30].

$$\eta_{ex} = 1 - \left(\frac{Ex_{D,tot}}{Ex_{QGeothermal} + Ex_{Recovery}}\right) \tag{10}$$

Tables 1 and 2 present the Rankine cycle exergy equations and the absorption cycle [31-34].

The electrolyzer relationships are presented in Table 3. To solve the system, first energy analysis and then exergy

analysis is performed for it. EES software has been used to solve thermodynamic equations.

RESULTS AND DISCUSSION

Validation of the present work using References [10] and [22] was used for the organic Rankin cycle with recovery and heating and electrolyzer systems. By comparing the references and the present work presented in Figs. 2 and 3, respectively, it can be seen that there is a good match between the results of the calculated parameters in the present work and the valid references.

Fig. 4 shows the performance characteristics of the system. All these values are calculated for four different operating fluids. It is observed that the operating fluid R245fa has the highest energy and exergy efficiency with 3.5% and 67.6%, respectively. Operating fluids R114, R600 and R236fa are also in the next categories in terms of performance characteristics. This paper also shows the lost exergy rate of system components for all operating fluids. Examining the system's exergy based on the above tables shows that the evaporator and the electrolyzer have the highest Exergy destruction (heat degradation) because

Table 1: Exergy rates of fuel and Rankine cycle product

Component name	Fuel Exergy	Product Exergy
Turbine	$E_6 - E_7$	W_{tur}
Superheater	$E_7 - E_8$	$E_{10} - E_9$
Condenser	$E_8 - E_1$	$E_{12} - E_{11}$
Pump	W_{pump}	$E_2 - E_1$
Recovery heat exchanger	$E_{14} - E_{13}$	$E_3 - E_2$
Economizer	$E_{17} - E_{18}$	$E_4 - E_3$
Evaporator	$E_{16} - E_{17}$	$E_5 - E_4$
Super Heater	$E_{15} - E_{16}$	$E_6 - E_5$

Table 2: Exergy rates of fuel and absorption cycle product.

Component name	Fuel Exergy	Product Exergy
Condenser	$E_{25} - E_{26}$	$E_{36} - E_{35}$
Liquid-steam heat exchanger	$E_{26} - E_{27}$	$E_{30} - E_{29}$
Expansion valve	E_{27}	E_{28}
Evaporator	$E_{28} - E_{29}$	$E_{34} - E_{33}$
Absorber	$E_{30} + E_{31} + E_{21}$	$E_{22} + E_{32}$
Pump	W_{pump}	$E_{23} - E_{22}$
Soluble heat exchanger	$E_{19} - E_{20}$	$E_{24} - E_{23}$
Generator	$E_{10} + E_{24}$	$E_9 + E_{19} + E_{25}$

Table 3: Relationships of proton membrane electrolyzers [20].

| Parameter	Equation
Electrolyzer voltage	$V = V_O + V_{act,c} + V_{act,a} + V_{ohm}$
Electrolyzer power consumption	$E_{electric} = JV, E_{electric} = W_{ORCT}$
Cathode activation potential	$V_{act,c} = \dfrac{RT}{F} \sinh^{-1}\left(\dfrac{J}{2J_{0,c}}\right), \qquad J_{0,c} = \int_c^{ref} \exp\left(\dfrac{-E_{act,c}}{RT}\right)$
Anode activation potential	$V_{act,a} = \dfrac{RT}{F} \sinh^{-1}\left(\dfrac{J}{2J_{0,a}}\right), \qquad J_{0,a} = \int_a^{ref} \exp\left(\dfrac{-E_{act,a}}{RT}\right)$
Ohmic potential	$V_{ohm} = JR_{PEM}, \qquad R_{PEM} = \int_0^D \dfrac{dx}{\sigma_{PEM}[\lambda(x)]}$ $\lambda(x) = \dfrac{\lambda_a - \lambda_c}{D}x + \lambda_c, \qquad \sigma_{FEM}[\lambda(x)] = [0.5139\lambda(x) - 0.326] \times \exp\left[1268\left(\dfrac{1}{303} - \dfrac{1}{T}\right)\right]$
Reversible potential	$V_O = 1.229 - 0.00085(T_{PEM} - 298)$
Molar flow rate of oxygen	$N_{H_2,out} = \dfrac{J}{2F} = N_{H_2O,reacted}$
Molar flow rate of oxygen	$N_{O_2,out} = \dfrac{J}{4F}$
Residual water flow rate	$N_{H_2O,out} = N_{H_2O,in} - \dfrac{J}{2F}$
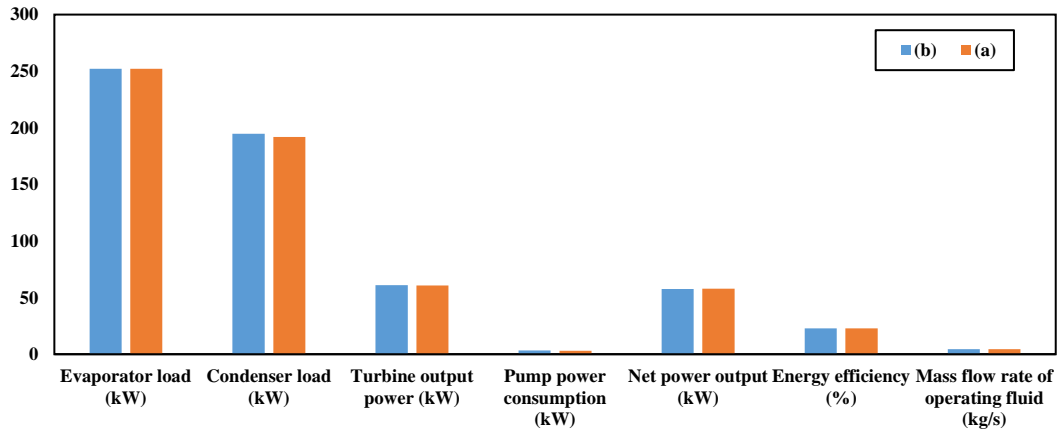
*Fig. 2: Performance parameters of organic Rankine cycle with feed fluid recovery and heating
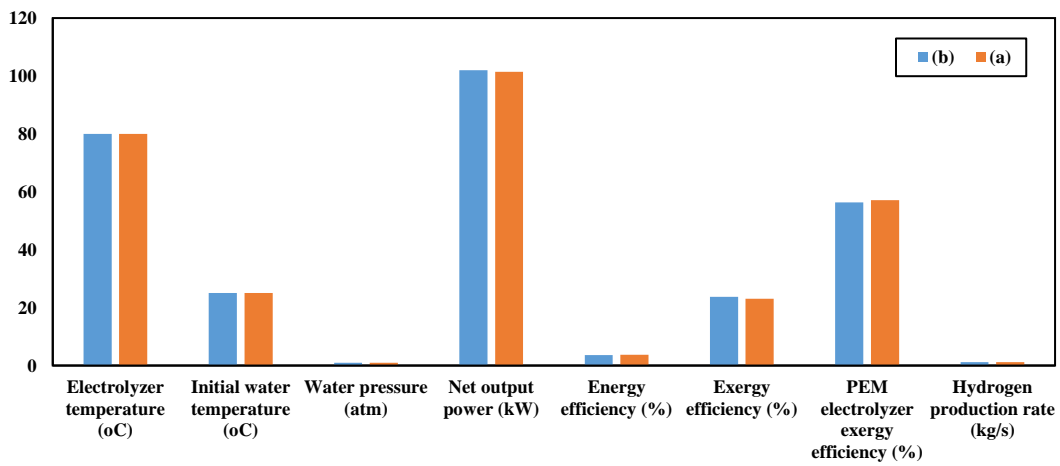a) The present model b) Reference [22].*

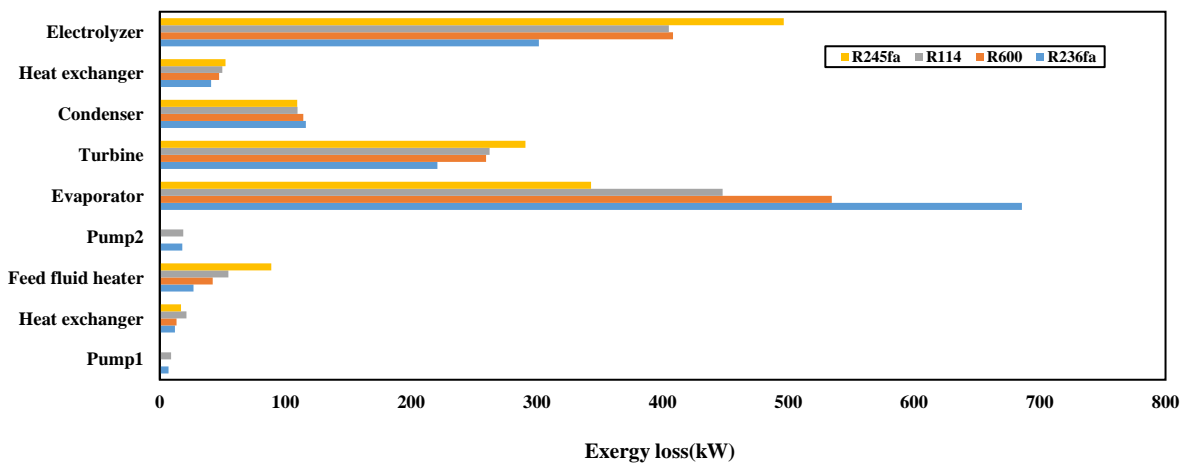*Fig. 3: Performance parameters of PEM electrolyzer system a) The present model b) Reference [10].*

Fig. 4: Loss of exergy rate of different system components.

Table 4: Changes in hydrogen production in terms of geothermal fluid temperature.

T_{Geo}	R236fa	R600	R114	R245fa
100	3.92	4.38	4.89	5.12
105	4.16	4.84	5.15	5.41
110	4.29	5.14	5.45	5.91
115	4.62	5.59	5.73	6.29
120	4.83	5.75	6.08	6.79
125	4.88	6.32	6.55	7.1
130	5.22	6.55	6.87	7.55
135	5.33	6.88	7.12	7.75
140	5.57	7.24	7.66	8.15
145	5.88	7.72	8.01	8.76
150	5.95	8.05	8.14	9.09
155	6.08	8.23	8.41	9.22
160	6.49	8.68	8.85	9.96
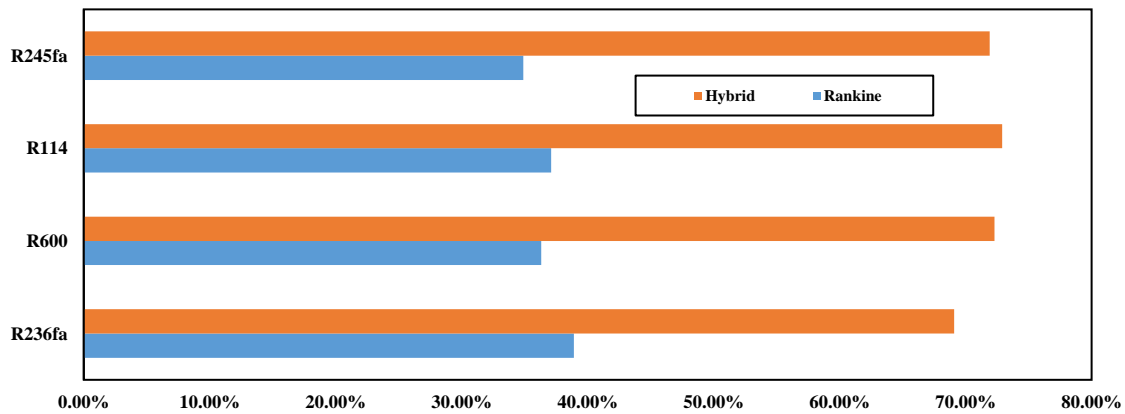
Fig. 5: Exergy efficiency of the plant with and without the hydrogen production plant.

both fuels' exergy flow rate is very high. It is also observed that with the change of operating fluid, as much as the exergy loss in the evaporator decreases, the exergy loss in the electrolyzer increases. This trend increases the power by reducing the loss of exergy in the evaporator. Comparing the operating fluids exegetically, it is observed that the operating fluid R245fa has the lowest exergy loss and the operating fluid R236fa has the highest extrusion loss in the evaporator, while the opposite is true in the electrolyzer (see Fig. 5). Therefore, it can be concluded that the operating fluid with less exergy loss in the evaporator produces more power and higher exergy loss in the electrolyzer.

To study the effect of geothermal fluid temperature changes on system performance, Table 4 shows the changes in hydrogen production and system output power in geothermal fluid temperature. It is observed that with increasing the temperature of the geothermal fluid, the system's output power shows a significant increase. By increasing the temperature of the geothermal fluid at the inlet of the evaporator, by keeping the outlet temperature and mass flow rate of the geothermal fluid, the difference between the enthalpy of the inlet and outlet increases, and by keeping the temperature of the operating fluid at the inlet and outlet of the evaporator, the mass flow rate increases. The output

power of the system and consequently the output power of hydrogen production also increases. Table 5 shows the changes in exergy efficiency concerning the temperature of the geothermal fluid. It is observed that with increasing the temperature of the geothermal fluid, the energy efficiency decreases. Although increasing the geothermal fluid temperature increases the output power, this increase also increases the system's heat and harms energy efficiency, according to the model. Besides, it is observed that the exergy efficiency also decreases. This trend is also due to the increase in the geothermal fluid's exergy flow at the evaporator inlet, which reduces the system's exergy efficiency[49-66]. To investigate the effect of change in geothermal fluid flow rate on system performance, Table 6 shows the hydrogen production changes in the geothermal fluid flow rate. It is observed that increasing the geothermal fluid flow rate has increased power and hydrogen production. Increasing the geothermal fluid flow rate increases the evaporator heat load, and due to the constant inlet and outlet temperatures of the operating fluid in the cycle to prevent the loss of this heat load, the operating fluid flow rate should be increased [67-89]. This process increases the system output power and consequently hydrogen production.

Table 7 shows the changes in exergy efficiency in geothermal fluid flow.

It is observed that increasing the flow rate of the geothermal fluid reduces energy efficiency and exergy. This trend is increasing the heat load of the evaporator, which reduces energy efficiency and exergy[89-100]. Comparing the effect of two factors, geothermal fluid temperature, and geothermal fluid flow, it is observed that with the change of geothermal fluid temperature, the performance characteristics of the system increase more, so the effect of geothermal fluid temperature on system performance is greater than the mass flow of geothermal fluid. Because with increasing the geothermal fluid temperature, the enthalpy of the geothermal fluid increases only at the evaporator inlet, while the output enthalpy is constant and increases the evaporator's heat load as the exergy current at the turbine inlet[31]. The enthalpy difference of the geothermal fluid does not affect the inlet and outlet of the evaporator, and consequently, the evaporator's heat load increases less, and the current exergy increases in addition to the inlet to the outlet of the evaporator. In the study of the effect of medium pressure (steam pressure is drawn from the turbine) on the system

Table 5: Changes in exergy efficiency of system in terms of geothermal fluid temperature.

T_{Geo}	R236fa	R600	R114	R245fa
100	63.4	69.1	69.78	66.97
105	63.95	67.31	67.09	66.27
110	61.33	65.92	65.64	64
115	60.83	63.32	64.88	64.99
120	59.01	62.42	65.13	63.45
125	58.64	61.71	62.56	62.83
130	56.99	61.31	61.92	60.79
135	55.33	60.48	60.28	58.99
140	54.68	58.82	60.33	59.71
145	53.55	57.98	58.24	56.66
150	53.01	56.53	58.76	56.47
155	51.17	55.99	56.93	55.75
160	49.92	55.05	56.73	53.59

Table 6: Changes in hydrogen production in the terms of the mass flow rate of geothermal fluid.

m_{brine}	R236fa	R600	R114	R245fa
50	2.02	2.5	2.73	3.07
55	2.27	2.8	2.96	3.4
60	2.52	3.04	3.15	3.66
65	2.79	3.31	3.36	3.93
70	2.96	3.48	3.59	4.12
75	3.29	3.77	3.87	4.34
80	3.42	3.98	4.17	4.63
85	3.73	4.14	4.32	4.83
90	3.88	4.53	4.54	5.1
95	4.22	4.68	4.82	5.39
100	4.39	4.86	5.06	5.42
105	4.62	5.15	5.37	5.73
110	4.92	5.49	5.46	5.91

performance in Table 8, changes in power and hydrogen production in terms of average pressure are shown. It can be seen that with the increase, the average mean pressure of the output work decreases. It is observed that from 500 kPa to 700 kPa, this decrease is small, and from the pressure of 700 kPa onwards, the slope decreases faster.

Table 9 shows the changes in energy efficiency and exergy in terms of mean pressure. the variation of output power and hydrogen production caused by any changes in the mean pressure is shown. It is observable that, in the pressure range of 500–700 kPa, there is a slight reduction in net output power with mean pressure augmentation. Afterward, this reduction is much greater. In other words, increasing the mean pressure enhances the extracted steam's enthalpy while decreasing the mass flow rate. Eventually, according to the model, it can be implied from the findings that these two factors have negative effects on power. Moreover, a decrease in output power will also reduce the electrolyzer's input energy, which gives a drop in the current density. Therefore, increasing the mean pressure will reduce hydrogen production.

It is observed that energy efficiency decreases with increasing average mean pressure [32]. The reason for this trend is the reduction of hydrogen production, which directly affects energy efficiency [33]. We also see an increase in exergy efficiency with increasing mean intermediate pressure. As the mean intermediate pressure increases, as mentioned earlier, the subducted vapor's enthalpy increases, and its mass fraction decreases. These two factors reduce the rate of fuel exergy flow in the turbine [34]. Besides, increasing the mean intermediate pressure reduces the power, and decreasing the power according to the relationships in Table 5 reduces fuel exergy in the electrolyzer [35]. The mentioned factors each have a positive effect on the exergy efficiency and increase the exergy efficiency [36]. It can be seen that at higher pressures, the operating fluid R114 has the highest exergy efficiency [37]. Table 9 shows the variation of total exergy and energy efficiencies resulting from varying the mean pressure value [38]. The implication is that increasing the mean pressure reduces energy efficiency. The main reason for this process is the reduction of hydrogen production, which directly influences energy efficiency [39]. Additionally, following an increase in the mean pressure, a higher exergy efficiency can be observed. As was stated before, a rise in the mean pressure will lead to a high

Table 7: Changes in exergy efficiency in terms of the mass flow rate of geothermal fluid.

m_{brine}	R236fa	R600	R114	R245fa
50	47.27	48.9	47.89	49.49
55	47.15	47.66	47.7	47.46
60	46.33	47.16	47.35	46.91
65	46.1	46.66	46.05	46.13
70	45.48	45.43	45.69	45.8
75	45.46	45.41	44.45	46
80	43.11	44.58	44.53	44.17
85	43.1	44.16	44.18	44.63
90	42.47	42.87	43.17	43.72
95	41.64	41.83	42.62	43.17
100	41.89	41.14	41.31	41.89
105	39.87	41.81	40.07	42.05
110	38.93	40.27	39.82	41.35

Table 8: Changes in hydrogen production in terms of average mean pressure.

P_{Mean}	R236fa	R600	R114	R245fa
100	2.61	3.84	3.99	4.44
105	2.61	3. 83	3.92	4.32
110	2.59	3.75	3.86	4.41
115	2.52	3.75	3.92	4.35
120	2.5	3.77	3.82	4.33
125	2.47	3.68	3.73	4.27
130	2.42	3.62	3.81	4.25
135	2.41	3.67	3.71	4.25
140	2.37	3.56	3.65	4.16
145	2.33	3.67	3.74	4.12
150	2.31	3.63	3.71	4.1
155	2.29	3.54	3.61	4.05
160	2.23	3.56	3.53	4

Table 9: Energy efficiency of the whole system in terms of average mean pressure.

P_{Mean}	R236fa	R600	R114	R245fa
100	63.81	68.84	68.74	69.14
105	63.83	69.42	70.75	68.12
110	65.32	68.68	70.48	69.79
115	65.15	70.73	71.02	69.21
120	66.6	69.44	71.04	70.29
125	66.04	70.46	71.37	70.88
130	65.68	70.67	71.61	71.6
135	67.7	70.25	70.8	69.88
140	67.1	71.66	72.09	72.3
145	66.74	72.85	71.46	70.57
150	68.22	71.22	74	73.28
155	66.97	73.4	74.66	71.48
160	67.17	72.6	72.98	73.99

enthalpy of extracted steam and a reduction in its mass fraction [40]. These two factors will reduce the flow rate of fuel exergy in the turbine [35, 37]. In addition, increasing the mean pressure results in a reduction of output power, and hence the fuel exergy flow rate in the electrolyzer will be reduced [39]. Each of the factors mentioned above has positive effects on exergy efficiency and can increase it. Moreover, it is indicated that at higher mean pressures, R114 has the highest exergy efficiency [40].

CONCLUSIONS

This research presented energy and exergy analysis of synchronous output power and hydrogen production system by integrating a regenerative organic Rankine cycle with a proton exchange membrane electrolyzer. A comprehensive thermodynamic modeling and parametric study were conducted for all selected working fluids. The significant results obtained from this study, a hybrid energy system is introduced to increase the system's overall performance by cogeneration of power and hydrogen. The hybrid system is based on an efficient organic Rankin cycle and a proton membrane exchange electrolyzer. Comprehensive thermodynamic modeling, a parametric

study has been performed for all operating fluids. This study's important results are that the operating fluid R245fa has the highest energy and exergy efficiency with 3.5% and 67.6%, respectively. The operating fluids R114, R600, and R236fa are also in the next categories in terms of performance characteristics. R245fa operating fluid has the least exergy loss, and R236fa was the operating fluid with the highest exergy loss in the evaporator, while this is the opposite in the electrolyzer. The operating fluid with less exergy loss in the evaporator produces more power and produces more exergy loss in the electrolyzer. As the geothermal fluid temperature increases, the production of power and hydrogen increases, but the energy and exergy efficiency decrease. As the mass flow rate of geothermal fluid increases, the production of power and hydrogen increases, but the energy and exergy efficiencies decrease. Increasing the mean intermediate pressure reduces power and hydrogen production and energy efficiency, but exergy efficiency increases.

Nomenclature

a	Anode
brine	Geothermal fluid
C	Condenser
c	Cathode
cold	Cold stream
evap	Evaporator
in	Inlet
out	Outlet
ohm	Ohmic
p	Pump
ref	working fluid
t	Turbine
P	Pressure, kPa
q	Specific heat, kJ/kg
Q	Heat rate, kW
s	Specific entropy, kJ/(kg.K)
T_0	Ambient temperature, K
V_0	Reversible potential, V
η	Efficiency, %
J	Current density, A/m^2
D	Thickness, μm
$E_{electrolyzer}$	Power to electrolyzer, kW
$E_{product}$	Power to the grid, kW
$E_{act,a/c}$	Anodic/cathodic activation energy, kJ/mol
F	Farady constant, C/mol

G	Gibbs free energy, J/mol
h	Specific enthalpy, kJ/(kg.K)
$J_{0,a/c}$	Exchange current density, A/m^2
J_i^{ref}	Potential factor of the anode and cathode
m	Mass flow rate, kg/s or kg/h
N	Molar flow, mol/s
R	Universal gas constant, kJ/(kg.K)
R_{PEM}	Ohmic resistance, Ω
T_{PEM}	Electrolyzer temperature, ºC or K
$T_{geo,mean}$	The average temperature of the geothermal fluid, K
$V_{act,a/c}$	Anode and cathode activator potential, V
σ	The conductivity of proton exchange membrane, s/m
λ	Water on the surface of the anode and cathode membrane, Ω^{-1}

REFERENCES

[1] Alhamid M. I., Daud Y., Surachman A., Sugiyono A., Aditya H.B., Mahlia T. M. I., Potential of Geothermal Energy for Electricity Generation in Indonesia: A Review, *Renewable and Sustainable Energy Reviews*, **53**: 733-740 (2016).

[2] Michaelides E.E.S., Future Directions and Cycles for Electricity Production from Geothermal Resources, *Energy Conversion and Management*, **107**: 3-9 (2016).

[3] Shokati N., Ranjbar F., Yari M., Exergoeconomic Analysis and Optimization of Basic, Dual-Pressure and Dual-Fluid Orcs and Kalina Geothermal Power Plants: A Comparative Study, *Renewable Energy*, **83**: 527-542 (2015).

[4] Braga L. B., Silveira J. L., Da Silva M. E., Tuna C. E., Machin E. B., Pedroso D. T., Hydrogen Production by Biogas Steam Reforming: A Technical, Economic and Ecological Analysis, *Renewable and Sustainable Energy Reviews*, **28**: 166-173 (2013).

[5] Ahmadi P., Dincer, I., Rosen M.A., Energy and Exergy Analyses of Hydrogen Production Via Solar-Boosted Ocean Thermal Energy Conversion and PEM Electrolysis, *International Journal of Hydrogen Energy*, **38(4)**: 1795-1805 (2013).

[6] Jiang L., Wang L.W., Liu C.Z., Wang R.Z., Experimental Study on a Resorption System for Power and Refrigeration Cogeneration, *Energy*, **97**: 182-190 (2016).

[7] Rahmouni S., Settou N., Chennouf N., Negrou B., Houari M., A Technical, Economic and Environmental Analysis of Combining Geothermal Energy with Carbon Sequestration for Hydrogen Production, *Energy Procedia*, **50**: 263-269 (2014).

[8] Bicer Y., Dincer I., Development of a New Solar and Geothermal Based Combined System for Hydrogen Production, *Solar Energy*, **127**: 269-284 (2016).

[9] Balta M. T., Dincer I., Hepbasli A., Exergoeconomic Analysis of a Hybrid Copper–Chlorine Cycle Driven by Geothermal Energy for Hydrogen Production, *International Journal of Hydrogen Energy*, **36(17)**: 11300-11308 (2011).

[10] Cai Q., Adjiman C. S., Brandon N.P., Optimal Control Strategies For Hydrogen Production when Coupling Solid Oxide Electrolysers with Intermittent Renewable Energies, *Journal of Power Sources*, **268**: 212-224 (2014).

[11] Mahmoudan A., Samadof P., Hosseinzadeh S., Garcia D.A., A Multigeneration Cascade System Using Ground-source Energy with Cold Recovery: 3E Analyses and Multi-objective Optimization, *Energy*, **233(15)**: 121185 (2021).

[12] Hoseinzadeh S., Yargholi R., Kariman H., Stephan Heyns P., Exergoeconomic Analysis and Optimization of Reverse Osmosis Desalination Integrated with Geothermal Energy, *Environmental Progress & Sustainable Energy*, **39(5)**: e13405 (2020).

[13] Sohani A., Shahverdian M. H., Sayyaadi H., Hoseinzadeh S., Memon S., Piras G., Astiaso Garcia D., Energy and Exergy Analyses on Seasonal Comparative Evaluation of Water Flow Cooling for Improving the Performance of Monocrystalline PV Module in Hot-Arid Climate, *Sustainability*, **13(11)**: 6084 (2021).

[14] Hoseinzadeh S., Stephan Heyns P., Advanced Energy, Exergy, and Environmental (3E) Analyses and Optimization of a Coal-Fired 400 MW Thermal Power Plant, *Journal of Energy Resources Technology*, **143(8)**: 082106 (2021).

[15] Kariman H., Hoseinzadeh S., Heyns P.S., Sohani A., Modeling and Exergy Analysis of Domestic MED Desalination with Brine Tank, *Desalination and Water Treatment*, **197**: 1-13 (2020).

[16] Ghazvini M., Sadeghzadeh M., Ahmadi M.H., Moosavi S., Pourfayaz F., Geothermal Energy Use in Hydrogen Production: A Review, *International Journal of Energy Research*, **43(14)**: 7823-7851 (2019).

[17] Ahmadi M.H., Banihashem S.A., Ghazvini M., Sadeghzadeh M., Thermo-Economic and Exergy Assessment and Optimization of Performance of a Hydrogen Production System by Using Geothermal Energy, *Energy & Environment*, **29(8)**: 1373-1392 (2018).

[18] Ahmadi M.H., Mehrpooya M., Pourfayaz F., Exergoeconomic Analysis and Multi Objective Optimization of Performance of a Carbon Dioxide Power Cycle Driven by Geothermal Energy with Liquefied Natural Gas as its Heat Sink, *Energy Conversion and Management,* **119**: 422-434 (2016).

[19] Sadaghiani M.S., Ahmadi M.H., Mehrpooya M., Pourfayaz F., Feidt M., Process Development and Thermodynamic Analysis of a Novel Power Generation Plant Driven by Geothermal Energy with Liquefied Natural Gas as Its Heat Sink, *Applied Thermal Engineering,* **133**: 645-658 (2018).

[20] Ghaebi H., Farhang B., Parikhani T., Rostamzadeh H., Energy, Exergy and Exergoeconomic Analysis of a Cogeneration System for Power and Hydrogen Production Purpose Based on TRR Method and Using Low Grade Geothermal Source, *Geothermics*, **71**: 132-145 (2018).

[21] Basaran A., Ozgener L., Investigation of the Effect of Different Refrigerants on Performances of Binary Geothermal Power Plants, *Energy Conversion and Management,* **76**: 483-498 (2013).

[22] Safarian S., Aramoun F., Energy and Exergy Assessments of Modified Organic Rankine Cycles (ORCs), *Energy Reports*, **1**: 1-7 (2015).

[23] Xu Y., Jiang N., Pan F., Wang Q., Gao Z., Chen G., Comparative Study on Two Low-Grade Heat Driven Absorption-Compression Refrigeration Cycles Based on Energy, Exergy, Economic and Environmental (4E) Analyses, *Energy Conversion and Management*, **133**: 535-547 (2017).

[24] Cui P., Yu M., Liu Z., Zhu Z., Yang S., Energy, Exergy, and Economic (3E) Analyses and Multi-Objective Optimization of a Cascade Absorption Refrigeration System for Low-Grade Waste Heat Recovery, *Energy Conversion and Management*, **184**: 249-261 (2019).

[25] Liu X., Yang X., Yu M., Zhang W., Wang Y., Cui P., Zhu Z., Ma Y., Gao J., Energy, Exergy, Economic And Environmental (4E) Analysis of an Integrated Process Combining CO_2 Capture and Storage, an Organic Rankine Cycle and an Absorption Refrigeration Cycle, *Energy Conversion and Management*, **210**: 112738 (2020).

[26] Altun A.F., Kilic M., Thermodynamic Performance Evaluation of a Geothermal ORC Power Plant, *Renewable Energy*, **148**: 261-274 (2020).

[27] Pili R., Eyerer S., Dawo F., Wieland C., Spliethoff H., Development of a Non-Linear State Estimator for Advanced Control of an ORC Test Rig for Geothermal Application, *Renewable Energy*, **161**: 676-690 (2020).

[28] Schifflechner C., Dawo F., Eyerer S., Wieland C., Spliethoff H., Thermodynamic Comparison of Direct Supercritical CO_2 and Indirect Brine-ORC Concepts for Geothermal Combined Heat and Power Generation, *Renewable Energy*, **161**: 1292-1302 (2020).

[29] Pan S.Y., Gao M., Shah K.J., Zheng J., Pei S.L., Chiang P.C., Establishment of Enhanced Geothermal Energy Utilization Plans: Barriers and Strategies, *Renewable Energy*, **132**: 19-32 (2019).

[30] Norouzi N., 4E Analysis and Design of a Combined Cycle with a Geothermal Condensing System in Iranian Moghan Diesel Power Plant, *International Journal of Air-Conditioning and Refrigeration*, **28(3)**: 2050022 (2020).

[31] Khajehpour H., Norouzi N., Bashash Jafarabadi Z., Valizadeh G., Hemmati M.H., Energy, Exergy, and Exergoeconomic (3E) Analysis Of Gas Liquefaction and Gas Associated Liquids Recovery Co-Process Based on the Mixed Fluid Cascade Refrigeration Systems, *Iranian Journal of Chemistry and Chemical Engineering (IJCCE),* **41(4):** 1391-1410(2021).

[32] Ajam M., Mohammadiun H., Dibaee Bonab M. H., Mohammadiun M., Energy, Exergy and Economic Analyses of a Combined Heat and Power Generation Systems with a Gas Turbine and a Horizontal Axis Wind Turbine, *Iranian Journal of Chemistry and Chemical Engineering (IJCCE)* (2021)[In Press].

[33] Bidar B., Shahraki F., Energy and Exergy-Economic Assessments of Gas Turbine Based CHP Systems: A Case Study of SPGC Utility Plant, *Iranian Journal of Chemistry and Chemical Engineering (IJCCE)*, **37(5)**: 209-223 (2018).

[34] Noorpoor A.R., Mazare F., Conventional and Advanced Exergetic and Exergoeconomic Analysis Applied to an Air Preheater System for Fired Heater (Case Study: Tehran Oil Refinery Company), *Iranian Journal of Chemistry and Chemical Engineering (IJCCE),* **37(4)**: 205-219 (2018).

[35] Khoshrou I., Jafari Nasr M. R., Bakhtari K., Exergy Analysis of the Optimized MSFD Type of Brackish Water Desalination Process, *Iranian Journal of Chemistry and Chemical Engineering (IJCCE)*, **36(6)**: 191-208 (2017).

[36] Norouzi N., The Pahlev Reliability Index: A Measurement for the Resilience of Power Generation Technologies Versus Climate Change, *Nuclear Engineering and Technology,* **53(5)**: 1658-1663 (2021).

[37] Fani M., Norouzi N., Ramezani M., Energy, Exergy, and Exergoeconomic Analysis of Solar Thermal Power Plant Hybrid with Designed PCM Storage, *International Journal of Air-Conditioning and Refrigeration*, **28(04)**:2050030 (2020).

[38] Norouzi N., 4E Analysis of a Fuel Cell and Gas Turbine Hybrid Energy System, *Biointerface Res. Appl. Chem.*, **11**: 7568-7579 (2021).

[39] Khajehpour H., Norouzi N., Shiva N., Folourdi R.M., Bahremani E.H., Exergy Analysis and Optimization of Natural Gas Liquids Recovery Unit, *International Journal of Air-Conditioning and Refrigeration*, **29(01)**: 2150005 (2021).

[40] Khajehpour H., Norouzi N., Fani M., An Exergetic Model for the Ambient Air Temperature Impacts on the Combined Power Plants and its Management Using the Genetic Algorithm, *International Journal of Air-Conditioning and Refrigeration*, **29(01)**: 2150008 (2021).

[41] Vessally E., Mohammadi S., Abdoli M., Hosseinian A., Ojaghloo P., Convenient and Robust Metal-Free Synthesis of Benzazole-2-Ones Through the Reaction of Aniline Derivatives and Sodium Cyanate in Aqueous Medium, *Iran. J. Chem. Chem. Eng. (IJCCE),* **39(5)**: 11-19 (2020).

[42] Gharibzadeh, F., Vessally, E., Edjlali, L., Es'haghi, M., Mohammadi, R., A DFT Study on Sumanene, Corannulene and Nanosheet as the Anodes in Li−Ion Batteries, *Iran. J. Chem. Chem. Eng.*, **39(6)**: 51-62 (2020).

[43] Afshar M., Khojasteh R.R., Ahmadi R., Nakhaei Moghaddam M., In Silico Adsorption of Lomustin Anticancer Drug on the Surface of Boron Nitride Nanotube, *Chem. Rev. Lett.*, **4**: 178-184 (2021).

[44] Vessally, E., Hosseinian, A., A Computational Study on the Some Small Graphene-Like Nanostructures as the Anodes in Na−Ion Batteries, *Iran. J. Chem. Chem. Eng.*, **40(3)**: 691-703 (2021).

[45] Hashemzadeh B., Edjlali L., Delir Kheirollahi Nezhad P., Vessally E., A DFT Studies on a Potential Anode Compound for Li-Ion Batteries: Hexa-Cata-Hexabenzocoronene Nanographen, *Chem. Rev. Lett.,* **4**: 232-238 (2021).

[46] Vessally E., Farajzadeh P., Najafi E., Possible Sensing Ability of Boron Nitride Nanosheet and its Al– and Si–Doped Derivatives for Methimazole drug by Computational Study, *Iran. J. Chem. Chem. Eng. (IJCCE),* **40(4)**: 1001-1011 (2021).

[47] Majedi S., Sreerama L., Vessally E., Behmagham F., Metal-Free Regioselective Thiocyanation of (Hetero) Aromatic C-H Bonds using Ammonium Thiocyanate: An Overview, *J. Chem. Lett.,* **1**: 25-31 (2020).

[48] Amani V., Zakeri M., Ahmadi R., Binuclear Nickel(II) Complex Containing 6-methyl-2,2'-Bipyridine and Chloride Ligands: Synthesis, Characterization, Thermal Analyses, and Crystal Structure Determination, *Iran. J. Chem. Chem. Eng. (IJCCE),* **39(2)**: 113-122 (2020).

[49] Salehi N., Vessally E., Edjlali L., Alkorta I., Eshaghi M., Nan@Tetracyanoethylene (n=1-4) Systems: Sodium salt vs Sodium Electride, *Chem. Rev. Lett.,* **3**: 207-217 (2020).

[50] Soleimani-Amiri S., Asadbeigi N., Badragheh S., A Theoretical Approach to New Triplet and Quintet (nitrenoethynyl) alkylmethylenes,(nitrenoethynyl) alkylsilylenes,(nitrenoethynyl) alkylgermylenes, *Iran. J. Chem. Chem. Eng. (IJCCE)*, **39(4)**: 39-52 (2020).

[51] Sreerama, L., Vessally, E., Behmagham, F., Oxidative Lactamization of Amino Alcohols: An Overview, *J. Chem. Lett.,* **1**: 9-18 (2020).

[52] Kamel M., Mohammadifard M., Thermodynamic and Reactivity Descriptors Studies on the Interaction of Flutamide Anticancer Drug with Nucleobases: A Computational View, *Chem. Rev. Lett.,* **4**: 54-65 (2021).

[53] Vessally E., Musavi M., Poor Heravi M.R., A Density Functional Theory Study of Adsorption Ethionamide on the Surface of The Pristine, Si and Ga and Al-Doped Graphene, *Iran. J. Chem. Chem. Eng. (IJCCE)*, **40(6)**: 1720-1736 (2021).

[54] Vakili M., Bahramzadeh V., Vakili M., A Comparative Study of SCN- Adsorption on the $Al_{12}N_{12}$, $Al_{12}P_{12}$, and Si and Ge -Doped $Al_{12}N_{12}$ Nano-Cages to Remove from the Environment, *J. Chem. Lett.,* **1**: 172-178 (2020).

[55] Mosavi M., Adsorption behavior of Mphentermine on the Pristine and Si, Al, Ga- Doped Boron Nitride Nanosheets: DFT Studies, *J. Chem. Lett.,* **1**: 164-171 (2020).

[56] Vessally E., Siadati S.A., Hosseinian A., Edjlali L., Selective Sensing of Ozone and the Chemically Active Gaseous Species of the Troposphere by Using the C20 Fullerene and Graphene Segment, *Talanta*, **162**: 505-510 (2017).

[57] Rabipour S., Mahmood E A., Afsharkhas M., Abbasi V., A Review on the Cannabinoids Impacts on Psychiatric Disorders, *Chem. Rev. Lett.*, **5**: 234-240 (2022).

[58] Siadati S.A., Vessally E., Hosseinian A., Edjlali L., Possibility of Sensing, Adsorbing, and Destructing the Tabun-2D-Skeletal (Tabun nerve agent) by C20 Fullerene and its Boron and Nitrogen Doped Derivatives, *Synthetic Metals,* **220**: 606-611 (2016).

[59] Rabipour S., Mahmood E.A., Afsharkhas M., Medicinal Use of Marijuana and its Impacts on Respiratory System, *J. Chem. Lett.*, **3**: 86-94 (2022).

[60] Cao Y., Soleimani-Amiri S., Ahmadi R., Issakhov A., Ebadi A.G., Vessally E., Alkoxysulfenylation of Alkenes: Development And Recent Advances, *RSC Advances*, **11**: 32513-32525 (2021).

[61] Vessally, E., Soleimani-Amiri, S., Hosseinian, A., Edjlali, L., Babazadeh, M., Chemical Fixation of CO2 to 2-aminobenzonitriles: A Straightforward Route to Quinazoline-2, 4 (1H, 3H)-Diones with Green and Sustainable Chemistry Perspectives, *J. CO₂ Util.,* **21**: 342-352 (2017).

[62] Arshadi S., Vessally E., Hosseinian A., Soleimani-amiri S., Edjlali L., Three-component Coupling of CO_2, Propargyl Alcohols, and Amines: An Environmentally Benign Access to cyclic and Acyclic Carbamates (A Review), *J. CO₂ Util.,* **21**: 108-118 (2017).

[63] Kassaee M.Z., Buazar F., Soleimani-Amiri S., Triplet germylenes with Separable Minima At ab Initio and DFT Levels, *Journal of Molecular Structure: THEOCHEM*, **866(1-3)**: 52-57 (2008).

[64] Kassaee M.Z., Aref Rad H., Soleimani Amiri S., Carbon–Nitrogen Nanorings and Nanoribbons: A Theoretical Approach for Altering the Ground States of Cyclacenes and Polyacenes, *Monatshefte für Chemie-Chemical Monthly,* **141(12)**: 1313-1319 (2010).

[65] Koohi M., Soleimani Amiri S., Haerizade B.N., Substituent Effect on Structure, Stability, and Aromaticity of Novel BnNmC20–(n+ m) Heterofullerenes, *Journal of Physical Organic Chemistry*, **30(11)**: e3682 (2017).

[66] Koohi M., Soleimani-Amiri S., Shariati M. Novel X- and Y-Substituted Heterofullerenes X 4 Y 4 C 12 Developed from the Nanocage C 20, where X= B, Al, Ga, Si and Y= N, P, As, Ge: a Comparative Investigation on their Structural, Stability, and Electronic Properties at DFT, *Structural Chemistry*, **29(3)**: 909-920 (2018).

[67] Soleimani- Amiri S., Singlet and Triplet Cyclonona-3, 5, 7- trienylidenes and their α, ά- halogenated Derivatives at DFT, *Journal of Physical Organic Chemistry*, **33(2)**: e4018 (2020).

[68] Soleimani-Amiri S., Identification of Structural, Spectroscopic, and Electronic Analysis of Synthesized 4-(5-Phenyl-1, 3, 4-Oxadiazol-2-Ylthio)-3-Methylbenzene-1, 2-Diol: A Theoretical Approach, *Polycyclic Aromat. Compd*, **41(3)**: 635-652 (2021).

[69] Poor Heravi M.R., Azizi B., Abdulkareem Mahmood E., Ebadi A.G., Ansari M.J., Soleimani-Amiri S., Molecular Simulation of the Paracetamol Drug Interaction with Pt-decorated BC3 Graphene-Like Nanosheet, *Molecular Simulation*, **48(6)**: 517-525 (2022).

[70] Ghazvini M., Sheikholeslami-Farahani F., Soleimani-Amiri S., Salimifard M., Rostamian R., Green Synthesis of Pyrido [2, 1-a] Isoquinolines and Pyrido [1, 2-a] Quinolines by Using ZnO Nanoparticles, *Synlett*, **29(04)**: 493-496 (2018).

[71] Soleimani- Amiri S., Shafaei F., Varasteh Moradi A., Gholami- Orimi F., Rostami Z., A Novel Synthesis and Antioxidant Evaluation of Functionalized [1, 3]-Oxazoles Using Fe3O4- Magnetic Nanoparticles, *Journal of Heterocyclic Chemistry*, **56(10)**: 2744-2752 (2019).

[72] Soleimani Amiri S., Green production and Antioxidant Activity Study of New Pyrrolo [2, 1- a] Isoquinolines, *J. Heterocyclic Chem.*, **57(11)**: 4057-4069 (2020).

[73] Samiei Z., Soleimani-Amiri S., Azizi Z., Fe₃O₄@ C@ OSO₃H as an Efficient, Recyclable Magnetic Nanocatalyst in Pechmann Condensation: Green Synthesis, Characterization, and Theoretical Study, *Molecular Diversity*, **25(1)**: 67-86 (2021).

[74] Taheri Hatkehlouei S.F., Mirza B., Soleimani-Amiri S., Solvent-Free One-Pot Synthesis of Diverse Dihydropyrimidinones/Tetrahydropyrimidinones Using Biginelli Reaction Catalyzed by Fe₃O₄@ C@ OSO₃H, *Polycyclic Aromat. Compd*, **42(4)**: 1341-1357 (2022).

[75] Amiri S.S., Ghazvini M., Khandan S., Afrashteh S., KF/Clinoptilolite@MWCNTs Nanocomposites Promoted a Novel Four-Component Reaction of Isocyanides for the Green Synthesis of Pyrimidoisoquinolines in Water, *Polycyclic Aromat. Compd*, 1-16 (2021).

[76] Zarei F., Soleimani-Amiri S., Azizi Z., Heterogeneously Catalyzed Pechmann Condensation Employing the HFe (SO₄) 2.4 H₂O-Chitosan Nano-Composite: Ultrasound-Accelerated Green Synthesis of Coumarins, *Polycyclic Aromat. Compd*, 1-18 (2021).

[77] Feizpour Bonab M., Soleimani-Amiri S., Mirza B., Fe₃O₄@ C@ PrS-SO₃H: A Novel Efficient Magnetically Recoverable Heterogeneous Catalyst in the Ultrasound-Assisted Synthesis of Coumarin Derivatives, *Polycyclic Aromat. Compd,* 1-16 (2022).

[78] Soleimani-Amiri S., Hossaini Z., Azizi Z., Synthesis and Investigation of Biological Activity of New Oxazinoazepines: Application of Fe₃O₄/CuO/ZnO@ MWCNT Magnetic Nanocomposite in Reduction of 4-Nitrophenol in Water, *Polycyclic Aromat. Compd,* 1-22 (2022).

[79] Khoshtarkib Z., Ebadi A., Alizadeh R., Ahmadi R., Aman V., Dichloridobis (phenanthridine-κN) Zinc (II), *Acta Crystallog.,* **E65(7)**: m739-m740 (2009).

[80] Salehi N., Chemical composition of the Essential oil from Aerial Parts of Achillea filipendulina Lam. from Iran, *J. Chem. Lett.,* **1**: 160-163 (2020).

[81] Amani V., Ahmadi R., Naseh M., Ebadi A., Synthesis, Spectroscopic Characterization, Crystal Structure and Thermal Analyses of Two Zinc (II) Complexes with Methanolysis of 2-Pyridinecarbonitrile as a Chelating Ligand, *JICS*, **14(3)**: 635-642 (2017).

[82] Iji M., Dass P. M., Shalbugau K. W., Penuel B. L., Synthesis and Characterization of Heterogeneous Catalysts from Magnetic Sand and Kaolin, *Journal of Chemistry Letters,* **1(3)**: 139-142 (2020)

[83] Ahmadi R., Khalighi A., Kalateh K., Amani V., Khavasi H. R., Catena-Poly [[(5, 5′-dimethyl-2, 2′-bipyridine-κ2N, N′) cadmium (II)]-di-µ-chlorido]. *Acta. Crystallog.*, **E64(10)**: m1233-m1233 (2008).

[84] Benhachem F.Z., Harrache D., Evaluation of Physico-Chemical Quality and Metallic Contamination Level of Epikarstic Seepage Waters in Forest Zone, *J. Chem. Lett.,* **1**: 59-62 (2020).

[85] Soleimani- Amiri S., Arabkhazaeli M., Hossaini Z., Afrashteh S., Eslami A.A., Synthesis of Chromene Derivatives *via* Three- Component Reaction of 4-hydroxycumarin Catalyzed by Magnetic Fe3O4 Nanoparticles in Water, *Journal of Heterocyclic Chemistry*, **55(1)**: 209-213 (2018).

[86] Soleimani- Amiri S., Hossaini Z., Arabkhazaeli M., Karami H., Afshari Sharif Abad S., Green Synthesis of Pyrimido- Isoquinolines and Pyrimido- Quinoline Using ZnO Nanorods as an Efficient Catalyst: Study Of Antioxidant Activity, *Journal of the Chinese Chemical Society*, **66(4)**: 438-445 (2019).

[87] Norouzi N., Dynamic Modeling of the Effect of Vehicle Hybridization Policy on Carbon Emission and Energy Consumption, *J. Chem. Lett*, **3**: 99-106 (2022).

[88] Soleimani- Amiri S., Hossaini Z., Azizi Z., Synthesis and investigation of Antioxidant and Antimicrobial Activity of New Pyrazinopyrroloazepine Derivatives Using Fe₃O₄/CuO/ZnO@MWCNT MNCs as Organometallic Nanocatalyst by New MCRs, *Appl. Organomet. Chem.*, **36(4)**: e6573 (2022).

[89] Karbakhshzadeh A., Majedi S., Abbasi V., Computational Investigation on Interaction Between Graphene Nanostructure BC₃ and Rimantadine Drug, *J. Chem. Lett.,* **3**: 108-113 (2022).

[90] Norouzi N., Ebadi A. G., Bozorgian A., Vessally E., Hoseyni S.J., Energy and Exergy Analysis of Internal Combustion Engine Performance of Spark Ignition for Gasoline, Methane, and Hydrogen Fuels, *Iran. J. Chem. Chem. Eng. (IJCCE),* **40(6)**: 1909-1930 (2021).

[91] Rabipour S., Mahmood E. A., Afsharkhas M., Abbasi V., Cannabinoids Impact on Cognition: A Review from the Neurobiological Perspective, *Chem. Rev. Lett.,* **6**: 7-14 (2023).

[92] Norouzi N., Ebadi A. G., Bozorgian A., Hoseyni S. J., Vessally E., Cogeneration System of Power, Cooling, and Hydrogen from Geothermal Energy: An Exergy Approach, *Iran. J. Chem. Chem. Eng. (IJCCE)*, **41(2)**: 706-721 (2022).

[93] Silas K., Musa Y.P., Habiba M.D., Effective Application of Jatropha Curcas Husk Activated ZnCl₂, *Chem. Rev. Lett.,* **5**: 153-160 (2022).

[94] Khezri A., Edjlali L., Eshaghi M., Vardini M.T., Basharnavaz H., A Novel [3-(4-methoxyphenyl)isoxazole-5-yl]-methanol Compound: Synthesis, *Chem. Rev. Lett.,* **5**: 113-118 (2022).

[95] Hoseyni S.J., Manoochehri M., Asli M.D., Synthesis and Crystal Structure of Dibromido{[(2-Pyridyl) methyl](p-ethylphenyl)amine}Zinc, *Chem. Rev. Lett.,* **5**: 99-105 (2022).

[96] Kadhim M.M., Mahmood E.A., Abbasi V., Poor Heravi M.R., Habibzadeh S., Mohammadi-Aghdam S., Soleimani-Amiri S., Theoretical Investigation of the Titanium—Nitrogen Heterofullerenes Evolved from the Smallest Fullerene, *J. Mol. Graph. Model.,* **117**: 108269 (2022).

[97] Porgar S., Rahmanian N., Phase Equilibrium for Hydrate Formation in the Methane and Ethane System and Effect of Inhibitors, *Chem. Rev. Lett.,* **5**: 2-11 (2022)..

[98] Kadhim M.M., Mahmood E.A., Abbasi V., Poor Heravi M.R., Habibzadeh S., Mohammadi-Aghdam S., Shoaei S.M., Theoretical Investigation of the Titanium—Nitrogen Heterofullerenes Evolved from the Smallest Fullerene, *J. Mol. Graph. Model.,* **117**: 108269 (2022).

[99] Avşar C., Tümük D., Ertunç S., Gezerman A.O., A Review on Ammono-Carbonation Reactions: Focusing on the Merseburg Process, *Chem. Rev. Lett.,* **5**: 83-91 (2022).

[100] Rabipour S., Mahmood E., Ebadi A., Bozorgian A., Vessally E., Asadi Z., Afsharkhas M., A Systematic Review of Therapeutic Potential of Illicit Drugs: A Narrative Overview of How Cannabinoids and Psychedelics Can be Used in Medicine, *Iran. J. Chem. Chem. Eng. (IJCCE)*, **41(3)**: 722-752 (2022).

[101] Bejan A., Tsatsaronis G., Moran M., Thermal Design and Optimization, New York, Wiley, (1996).

[102] Elliot D., Huang S., Chen J.J., Lee R.J., Yao J., Zhang Y., Benefits of Integrating NGL Extraction and LNG liquefaction Technology, *AIChE Journal.*, (2005).

[103] Ahmadi N., Rezazadeh S., Dadvand A., Mirzaee I., Study of the Effect of Gas Channels Geometry on the Performance of Polymer Electrolyte Membrane Fuel Cell, *Periodica Polytechnica Chemical Engineering*, **62(1)**: 97-105 (2018).

[104] Ahmadi N., Rezazadeh S., Dadvand A., Mirzaee I., Modelling of Gas Transport in Proton Exchange Membrane Fuel Cells, *Proceedings of the Institution of Civil Engineers-Energy*, **170(4)**: 163-179 (2017).

[105] Ahmadi N., Kõrgesaar M., Analytical Approach to Investigate the Effect of Gas Channel Draft Angle on the Performance of PEMFC and Species Distribution, *International Journal of Heat and Mass Transfer*, **152**, (2020).

[106] Finn A.J., Developments in Natural Gas Liquefaction, *Hydrocarbon Process*, 47−59 (1999).

[107] Norouzi N., The Pahlev Reliability Index: A Measurement for the Resilience of Power Generation Technologies Versus Climate Change, *Nuclear Engineering and Technology* (2020).

[108] Norouzi N., Fani M., Talebi S., Exergetic Design and Analysis of a Nuclear SMR Reactor Tetrageneration (Combined Water, Heat, Power, and Chemicals) with Designed PCM Energy Storage and a CO2 Gas Turbine Inner Cycle, *Nuclear Engineering and Technology*, **53**: 677–687 (2021).

[109] Norouzi N., Hosseinpour M., Talebi S., Fani M., A 4E Analysis of Renewable Formic Acid Synthesis from the Electrochemical Reduction of Carbon Dioxide and Water: Studying Impacts of the Anolyte Material on the Performance of the Process, *Journal of Cleaner Production*, **293**, (2021).

[110] Khajehpour H., Norouzi N., Shiva N., Folourdi R. M., Bahremani E. H., Exergy Analysis and Optimization of Natural Gas Liquids Recovery Unit, *International Journal of Air-Conditioning and Refrigeration*, **29**, (2021).

[111] Norouzi N., Shiva N., Khajehpour H., Optimization of Energy Consumption in the Process of Dehumidification of Natural Gas, *Biointerface Research in Applied Chemistry*, **11**: 14634–14639 (2021).

[112] Norouzi N., Talebi S., Fani M., Khajehpour H., Exergy and Exergoeconomic Analysis of Hydrogen and Power Cogeneration Using an HTR Plant, *Nuclear Engineering and Technology* (2021).

[113] Norouzi N., Khajehpour H., Simulation of Methane Gas Production Process from Animal Waste in a Discontinuous Bioreactor, *Biointerface Research in Applied Chemistry*, **11**: 13850–13859 (2021).

[114] Norouzi N., Talebi S., Najafi P., Thermal-Hydraulic Efficiency of a Modular Reactor Power Plant by Using the Second Law of Thermodynamic, *Annals of Nuclear Energy*, **151**: 107936 (2021).

[115] Khajehpour H., Norouzi N., Fani M., An Exergetic Model for the Ambient Air Temperature Impacts on the Combined Power Plants and its Management Using the Genetic Algorithm, *International Journal of Air-Conditioning and Refrigeration*, **29(1)**: 2150008 (2021).

[116] Fani M., Norouzi N., Ramezani M., Energy, Exergy, and Exergoeconomic Analysis of Solar Thermal Power Plant Hybrid with Designed PCM Storage, *International Journal of Air-Conditioning and Refrigeration*, **28(4)**: 2050030 (2020).

[117] Gallo W.L.R. et al., Exergy Analysis of the Compression Systems and its Prime Movers for a FPSO unit, *Journal of Natural Gas Science and Engineering*, **44**: 287–298 (2017).

[118] Arnaiz del Pozo C., Jiménez Álvaro Á., Rodríguez Martín J., López Paniagua I., Efficiency Evaluation of Closed and Open Cycle Pure Refrigerant Cascade Natural Gas Liquefaction Process through Exergy Analysis, *Journal of Natural Gas Science and Engineering*, **89**: (2021).

[119] Ghorbani B., Ebrahimi A., Rooholamini S., Ziabasharhagh M., Pinch and Exergy Evaluation of Kalina/Rankine/Gas/Steam Combined Power Cycles for Tri-Generation of Power, Cooling and Hot Water Using Liquefied Natural Gas Regasification, *Energy Conversion and Management,* **223**: 113328 (2020).

[120] Zhang S. et al., Comprehensive Comparison of Enhanced Recycle Split Vapour Processes for Ethane Recovery, *Energy Reports*, **6**: 1819–1837 (2020).

[121] Mehrpooya M., Vatani A., Moosavian S., Optimum Pressure Distribution in Design of Cryogenic NGL Recovery Processes, *Iran. J. Chem. Chem. Eng. (IJCCE),* **31(3)**: 97-109 (2012).

[122] Ahmadi S., Nasr R., Comparative Study and Multi-Objective Optimization of Various Configurations in Natural Gas Liquefaction Process, *Iran. J. Chem. Chem. Eng. (IJCCE)*, **39(1)**: 313-336 (2020).

[123] Azari A., Shariaty-Niassar M., Alborzi M., Short-term and Medium-term Gas Demand Load Forecasting by Neural Networks, *Iran. J. Chem. Chem. Eng. (IJCCE)*, **31(4)**: 77-84 (2012).

[124] Norouzi N., 4E Analysis and Design of a Combined Cycle with a Geothermal Condensing System in Iranian Moghan Diesel Power Plant, *International Journal of Air-Conditioning and Refrigeration,* **28(3)**: 2050022 (2020).

[125] Garousi Farshi L., Mahmoudi S.M.S., Rosen M.A., Exergoeconomic Comparison of Double Effect and Combined Ejector-double Effect Absorption Refrigeration Systems, *Applied Energy*, **103**: 700–711 (2013).

[126] Ghorbani B., Salehi G.R., Amidpour M., Hamedi M.H., Exergy and Exergoeconomic Evaluation of Gas Separation Process, *Journal of Natural Gas Science and Engineering*, **9**:86-93 (2012).

[127] Morosuk T., Tesch S., Hiemann A., Tsatsaronis G., Bin Omar N., Evaluation of the PRICO Liquefaction Process using Exergy-based Methods, *Journal of Natural Gas Science and Engineering*, 1-9 (2015).

[128] Siddiqui F.R., El-Shaarawi M.A.I., Said S.A.M, Exergoeconomic Analysis of a Solar Driven Hybrid Storage Absorption Refrigeration Cycle, Energy Conversion and Management, **80**:165-172 (2014).

[129] Vatani A., Mehrpooya M., Palizdar A., Energy and Exergy Analyses of Five Conventional Liquefied Natural Gas Processes, *International Journal of Energy Research,* **38**:1843-1863 (2014).

[130] Azizkhani A., Gandomkar A., A Novel Method for Application of Nanoparticles as Direct Asphaltene Inhibitors During Miscible CO2 Injection, *Journal of Petroleum Science and Engineering*, **185** (2020).

[131] Pellegrini L.A., De Guido G., Valentina V., Energy and Exergy Analysis of Acid Gas Removal Processes in the LNG Production Chain, *Journal of Natural Gas Science and Engineering,* **61**: 303–319 (2019).

[132] Najibullah Khan N. B., Barifcani A., Tade M., Pareek V., A Case Study: Application of Energyand Exergy Analysis for Enhancing the Process Efficiency of a Three Stage Propane Pre-Cooling Cycle of the Cascade LNG Process, *Journal of Natural Gas Science and Engineering,* **29**: 125–133 (2016).

[133] Ghorbani B., Salehi G.R., Ghaemmaleki H., Amidpour M., Hamedi M.H., Simulation and Optimization of Refrigeration Cycle in NGL Recovery Plants With Exergy-Pinch Analysis, *Journal of Natural Gas Science and Engineering,* **7**: 35–43 (2012).

[134] Bidar B., Shahraki F., Energy and Exergo-Economic Assessments of Gas Turbine Based CHP Systems: A Case Study of SPGC Utility Plant, *Iran. J. Chem. Chem. Eng. (IJCCE)*, **37(5)**: 209-223 (2018).

[135] Noorpoor A., Mazare F., Conventional and Advanced Exergetic and Exergoeconomic Analysis Applied to an Air Preheater System for Fired Heater (Case Study: Tehran Oil Refinery Company), *Iran. J. Chem. Chem. Eng. (IJCCE)*, **37(4)**: 205-219 (2018).

[136] Khoshrou I., Jafari Nasr M., Bakhtari K. Exergy Analysis of the Optimized MSFD Type of Brackish Water Desalination Process, *Iran. J. Chem. Chem. Eng. (IJCCE)*, **36(6)**: 191-208 (2017).

[137] Norouzi N., 4E Analysis of a Fuel Cell and Gas Turbine Hybrid Energy System, *Biointerface Research in Applied Chemistry*, **11**: 7568-7579 (2021).

[138] Zaresharif M., Vatani A., Ghasemian M., Evaluation of Different Flare Gas Recovery Alternatives with Exergy and Exergoeconomic Analyses, *Arabian Journal for Science and Engineering*, **47**: 5501-5520 (2021).

[139] Hajizadeh A., Mohamadi-Baghmolaei M., Azin R., Osfouri S., Heydari I., Technical and Economic Evaluation of Flare Gas Recovery in a Giant Gas Refinery, *Chemical Engineering Research and Design*, **131(1)**: 506-519 (2018).

[140] Sabbagh O., Fanaei M.A., Arjomand A., Optimal Design of a Novel NGL/LNG Integrated Scheme: Economic and Exergetic Evaluation, *Journal of Thermal Analysis and Calorimetry*, **18**: 1-6 (2020).

[141] Abdulrahman I., Máša V., Teng S.Y., Process Intensification in the Oil and Gas Industry: A Technological Framework, *Chemical Engineering and Processing-Process Intensification*, **2**: 108208 (2020).

[142] Norouzi N., Talebi S., Fabi M., Khajehpour H., Heavy Oil Thermal Conversion and Refinement to the Green Petroleum: a Petrochemical Refinement Plant Using the Sustainable Formic Acid for the process, *Biointerface Research in Applied Chemistry*, **10**: 6088–6100 (2020).

[143] Norouzi N., Kalantari G., Talebi S., Combination of Renewable Energy in the Refinery, with Carbon Emissions Approach, *Biointerface Research in Applied Chemistry*, **10**: 5780-5786 (2020).

[144] Norouzi N., Talebi S., Exergy, Economical and Environmental Analysis of a Natural Gas Direct Chemical Looping Carbon Capture and Formic Acid-Based Hydrogen Storage System, *Iran. J. Chem. Chem. Eng. (IJCCE)*, **41(4):** 1436-1457 (2022).

[145] Norouzi N., Hydrogen Production in the Light of Sustainability: A Comparative Study on the Hydrogen Production Technologies Using the Sustainability Index Assessment Method, *Nuclear Engineering and Technology*, **54(4)**: 1288-1294 (2021).